Geographic Optimal Transport for Heterogeneous Data: Fusing Remote Sensing and Social Media

Zhenjie Liu, *Member, IEEE*, Qiang Qiu, Jun Li, *Senior Member, IEEE*, Lizhe Wang, and Antonio Plaza, *Fellow, IEEE*

***Abstract*— The fusion of heterogeneous remote sensing and social media data can fill the gaps in satellite image collections and improve the spatiotemporal resolution of the available data sets. As a result, it is being gradually adopted in multimodal data analytics. Generally, the fusion of heterogeneous geographic data faces the following issues: 1) the probability density functions may differ from different data sources and 2) the geolocations may not be well aligned. The former one can be generally solved by performing an alignment of representations in the source and target domains using, for instance, domain adaptation. The latter issue is seldom considered in the fusion of heterogeneous geographic data. In this article, we present a new method called geographic optimal transport (GOT), which aims at aligning representations and geolocations in a simultaneous fashion. A flood event that took place in 2013 in Boulder, CO, USA, is taken as a case study to evaluate our GOT method. Here, we consider two remote sensing features derived from water indicators, i.e., the normalized difference vegetation index (NDVI) and the normalized difference water index (NDWI), for the fusion of Landsat 8 imagery and Twitter data. A comparison between our newly developed GOT and the traditional optimal transport (OT) is performed. Experimental results demonstrate that the proposed GOT can accurately align spatially biased georeferenced tweets to the flood phenomena, leading to the conclusion that GOT can effectively fuse heterogeneous remote sensing and social media data.**

***Index Terms*— Data fusion, geolocation alignment, remote sensing, representation alignment, social media.**

I. Introduction

With the advent of the big data era, the limitations of using a single data source are obvious in many research fields [1]–[3]. Researchers are driven to describe and analyze an event in a way that is as detailed as possible, as multimodal data analysis exhibits significant advantages and potential. Thus, it is better to rely on data recorded by several sensors rather than by one sensor only. Therefore, multiple data sources are important in many applications, resulting in the fact that the collection and analysis of multimodal data have gradually attracted widespread attention.

The fusion of multimodal data can better account for geographic phenomena and provide more accurate and reliable information in events [3], [4]. However, since multimodal data sensed from various devices are heterogeneous, the fusion of multimodal data generally suffers from two issues: 1) the probability density functions may differ in different data sources [5], [6] and 2) the geolocations may not be well aligned [7], [8]. To address the former problem (i.e., probability density functions are different), models built from one domain generally do not fit another domain. As a result, they cannot accomplish the same tasks in other domains. Domain adaptation has been widely used to solve that specific problem in the literature. This approach aims at reducing the differences between data distributions of the source and target domains, aligning their representations [9]–[14]. Optimal transport (OT) has been recently introduced as a highly effective domain adaptation technique, which reduces the divergence between the source and the target probability measures by minimizing the Wasserstein distance [15]. This technique has achieved remarkable results in different problems [5], [16].

Concerning the problem of geolocations, for the same entity, its geolocation in one domain is different from its location in another domain. Therefore, to fuse remote sensing data, it is important to take the problem of geolocations into account. A possible solution is to map multisource layers to the same coordinate space through spatial transformations [17]–[19]. For example, the registration between multisource images is a typical application of geolocation alignment, e.g., the alignment of homogeneous Landsat and Sentinel-2 images [20] or the alignment of heterogeneous Landsat and Sentinel-1 images [21]. However, it should be pointed out that there are very few studies analyzing the problem of geolocations in the context of fusing remote sensing data with social sources of geographic data, for example, social media data.

The popularity of social media (and the proliferation of their users) has led to an increasingly interconnected world. Social media with global positioning system (GPS) functions have become highly innovative geographic data sources provided by many applications, such as Twitter, Instagram, Flickr,

Manuscript received May 4, 2020; revised August 29, 2020; accepted September 23, 2020. This work was supported by the Strategic Priority Research Program of the Chinese Academy of Sciences under Grant XDA19090104. *(Corresponding author: Jun Li.)*

Zhenjie Liu and Jun Li are with the Guangdong Provincial Key Laboratory of Urbanization and Geo-Simulation, School of Geography and Planning, Sun Yat-sen University, Guangzhou 510275, China (e-mail: lijun48@mail.sysu.edu.cn).

Qiang Qiu is with the Institute of Computing Technology, Chinese Academy of Sciences, Beijing 100190, China.

Lizhe Wang is with the School of Computer Science, China University of Geosciences, Wuhan 430074, China.

Antonio Plaza is with Hyperspectral Computing Laboratory, Department of Technology of Computers and Communications, Escuela Politécnica, University of Extremadura, 10071 Cáceres, Spain.

Color versions of one or more of the figures in this article are available online at http://ieeexplore.ieee.org.

Digital Object Identifier 10.1109/TGRS.2020.3031337

Facebook, and Weibo. This type of social media data is defined as voluntary geographic information (VGI) and uses "citizens as sensors" [22] to capture microscopic real-time geographic data in the form of text, images, and videos. The extensive coverage and real-time nature of social media data provides great added value for improving the situational awareness of ongoing events [23], [24].

Despite the wide availability of existing satellite images, due to satellite revisit limitations, specific data may not be available at the most urgent time and place. This means that there may be missing data (gaps) from the viewpoint of data availability. Therefore, the fusion of heterogeneous remote sensing data and social media data can help fill these gaps in satellite image collections and improve the spatiotemporal resolution of the available data sets [25], [26]. This research topic has attracted widespread attention in recent years [3], [27]–[29]. For example, Panteras and Cervone [30] performed geostatistical analysis of daily Twitter data in order to enhance the spatiotemporal resolution of the flood extent retrieved by multisource remote sensing satellites, including Earth Observing-1 (EO-1), Landsat 8, WorldView-2, and WorldView-3. However, existing studies on the fusion of remote sensing and social media data mainly focus on the alignment of the representations, assuming that there are no problems concerning geolocations (i.e., it is always assumed that the geolocations indicated by geographic entities are consistent with corresponding geographic phenomena). In fact, this assumption may not hold in real scenarios, and there may be (intentional or unintentional) problems with geolocations when geographic data are generated [7], [31]. Taking a flood event as an example, the geolocations indicated by the geotagged messages are the locations of the social media users, which usually correspond to relatively safe places (and not always the exact inundated places). To address this issue, Wang *et al.* [31] directly applied the OT method to relocate spatially biased georeferenced tweets to the historical flood areas, combined with Landsat images collected before and after the disaster.

Although the OT algorithm is able to solve problems caused by different probability density functions and further align representations, it may not be appropriate to address problems concerning the geolocations of geographic entities and geographic phenomena. In fact, OT minimizes the overall transportation cost to achieve domain adaptation, predefining the weights of each location in the target domain following a uniform distribution. However, a location with more tweeters is likely to have more data, whereas a location with a few tweeters probably has less data. Therefore, it is unlikely that the data are produced with a uniform distribution, which leads to the conclusion that OT exhibits clear limitations when aligning geographic entities and indicated geographic phenomena.

In this article, we develop a new alignment method called geographic optimal transport (GOT) that is able to tackle problems related to both probability density functions and geolocations (simultaneously) in the context of heterogeneous remote sensing and social media data fusion. In order to illustrate the advantages of our method, we consider a flood event that took place in 2013 in Boulder, CO, USA, as a case study. Specifically, we focus on the problem of fusing remote sensing images collected from the Landsat 8 operational land imager (OLI) satellite and geotagged tweets of this event. In order to accomplish the fusion task, remote sensing features derived from water indicators, i.e., the normalized difference vegetation index (NDVI) and the normalized difference water index (NDWI are plugged into the proposed GOT, leading to more effective alignments of Landsat 8 OLI images and tweets in the considered case study. The main innovative contributions of our work are as follows:

1) a new fusion method, named GOT, for the fusion of heterogeneous geographic data (aimed at simultaneously aligning representations and geolocations);
2) for the considered flood event case study, a careful investigation of NDVI and NDWI remote sensing features and the development of two new forms of features: NDWI difference and NDVI difference (considering the times before and after flood);
3) a new metric, named corrected precision "P_c," for the evaluation of the performance of geolocation alignments.

The rest of this article is organized as follows. Section II discusses some related works. Section III describes our newly proposed GOT method. Section IV describes the data sets used in our study. Section V describes our experimental results. Section VI concludes this article with some remarks and hints at plausible future research lines.

II. Related Works

In this section, we review the existing literature on domain adaptation and OT.

A. Domain Adaptation

In order to solve the issues related to probability density functions and perform alignment of representations, domain adaptation has been widely adopted to transfer knowledge from a source domain to a target domain. Domain adaptation can be divided into two main categories, i.e., semisupervised and unsupervised approaches. Semisupervised domain adaptation uses labels in the target domain, whereas unsupervised domain adaption does not use any labels from the target domain.

There are many works developed for semisupervised domain adaptation. A first attempt is to learn a domain-invariant feature space by using all labeled samples, both from the source and target domains. For instance, in [9], a linear transformation is formed to map features from the target (test) domain to the source (training) domain for representation learning. In [10], the effect of domain-induced changes in the feature distribution is minimized for transfer learning. In [11], a flexible model for learning nonlinear transformations between the domains is proposed for transferring object models from one data set to another. In [32], a kernel-based manifold alignment method is proposed for the construction of a common, semantically meaningful representation domain, aiming at the matching of an arbitrary number of data sources. Wang and Mahadevan constructed mappings to link different feature spaces in order

to transfer knowledge across domains. In addition, some studies use the target labels to adapt the source labeled information, so that noise and outliers in the source labels can be removed for mapping purposes, resulting in a more robust model. For instance, Jhuo *et al.* [34] proposed a low-rank method to reconstruct the source samples by the targets, reducing the domain distribution disparity.

Unsupervised domain adaptation attracted more attention recently, as it does not require labeled information from the targets (in real scenarios, and it is generally difficult to obtain labels from the target domain). In order to achieve unsupervised domain adaption, an intuitive solution is to map both the source and the target to a joint feature space. For instance, Pan *et al.* [12] proposed a novel dimensionality reduction framework for reducing the distance between domains in a latent space for domain adaptation purposes. In [35], a projection is learned to map data instances from different spaces to a lower dimensional space, simultaneously matching the local geometry and preserving the neighborhood relationship within each set. In [36], a new deep network-based approach is proposed to jointly learn transferable features from labeled data in the source domain and unlabeled data in the target domain. In [37], a domain-invariant projection approach is introduced to project the data to a low-dimensional latent space, where the distance between the empirical distributions of the source and target examples is minimized. In [38], generative subspaces are created from both the source and target domains. Apart from learning a joint feature space, another straightforward solution for unsupervised domain adaption is to project the source to the target. For instance, Saito *et al.* [39] aligned the distributions of the source and the target by utilizing task-specific decision boundaries.

B. Optimal Transport

OT, which can be performed in both semisupervised and unsupervised mode, has been recently proved to be an effective domain adaptation technique. For instance, in [5], a regularized unsupervised OT model is proposed to match both probability density functions of the source and target domains, constraining labeled samples of the same class in the source domain to remain close during transport. In [40], a regularized OT-based unsupervised domain adaptation approach is proposed to find an optimal mapping from training to test samples by minimizing the distribution inconsistencies between the source and target domains. In [41], OT was exploited for semisupervised heterogeneous domain adaptation, which preserves the semantic consistency between heterogeneous domains in which target and transported source samples with the same label are enforced to follow similar distributions. In [31], an OT-based domain adaptation technique was introduced for the fusion of heterogeneous remote sensing and social media data, with the goal of detecting (and predicting) weather-driven natural hazards.

III. Methodology

This section introduces the proposed GOT method for the fusion of heterogeneous remote sensing and social media data.

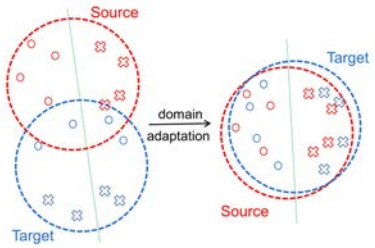

Fig. 1. Graphical illustration of domain adaptation, where two domains, i.e., a source domain and a target domain, are considered. There are eight elements, with four belonging to the "cross" class and four belonging to the "circle" class, respectively.

A. Domain Adaptation

Let us assume that there are K different geographic data modalities, represented as maps $\{f_k\}_{k=1,\ldots,K}$, with domains D_k and ranges $\mathbb{V}_k$, respectively

$$f_k : D_k \to \mathbb{V}_k. \tag{1}$$

With this definition in mind, the goal of domain adaptation is to align representations and homogenize the domains of different geographic data modalities (D_k) into a common space $D = \{x_1, \ldots, x_n\}$ with $x_i \in \mathbb{R}^2$, for $i = 1, \ldots, n$, being its element

$$\phi_k : D_k \to D. \tag{2}$$

Fig. 1 shows a graphical illustration of the concept of domain adaptation. In this graph, two domains, i.e., a source domain (in red) and a target domain (in blue), are considered. In both domains, there are eight elements: four belonging to a so-called "cross" class and four belonging to a "circle" class, respectively. As it can be observed in the graph, it is very difficult to separate the two classes in the original domains. After domain adaption, the source domain and the target are aligned so that the two classes can be well separated in the joint domain.

B. Optimal Transport Algorithm

The traditional OT algorithm offers a way to find a minimal effort solution to transport the distribution in the source domain to the target domain. The space of the source distribution and the target distribution can be, respectively, denoted by $D_s = \{x_1^s, \ldots, x_{n_s}^s\}$ and $D_t = \{x_1^t, \ldots, x_{n_t}^t\}$, with n^s and n^t being the number of elements in D_s and D_s.

Let Σ be the σ-algebra on $D = \{x_1, \ldots, x_n\}$, and $\mathcal{P}(D)$ denote the space of probability measures over Σ. The source distribution $P_s \in \mathcal{P}(D)$ (e.g., the biased tweets) and the target distribution $P_t \in \mathcal{P}(D)$ (e.g., the historical flood areas) can be, respectively, written as

$$\begin{aligned} P_s &= \sum_{x_i \in D} a_i^s \delta_{x_i} \\ P_t &= \sum_{x_i \in D} a_i^t \delta_{x_i} \end{aligned} \tag{3}$$

where δ_{x_i} is the Dirac unit mass at location x_i and a_i's, a_i^s's, and a_i^t's are the coefficients in the probability simplex Σ_n, i.e., $\sum_{i=1}^n a_i = 1$, $\sum_{i=1}^n a_i^s = 1$, and $\sum_{i=1}^n a_i^t = 1$.

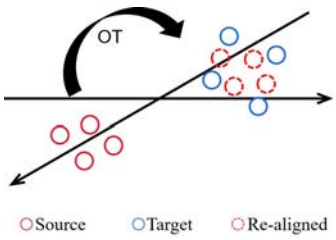

Fig. 2. Graphic illustration of OT from the viewpoint of representation alignment. There are four source elements (in red) and four target elements (in blue), respectively.

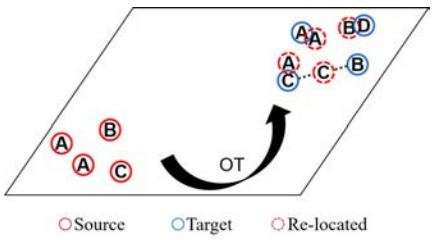

Fig. 3. Graphic illustration of domain adaption results in Fig. 2 in view of the geolocation of the elements, where "A," "B," "C," and "D" represent geographical phenomena, {"A," "A," "B," "C"} (in rxed) are collected by the source, and {"A," "B," "C," "D"} are collected by the target.

In the case of the discrete OT, the empirical distributions $\widehat{P}_s$ and $\widehat{P}_t$ are the estimations of P_s and P_t through discrete samples in the source and target distribution, respectively

$$\widehat{P}_s = \sum_{i=1}^{n_s} \hat{a}_i^s \delta_{x_i^s}$$
$$\widehat{P}_t = \sum_{i=1}^{n_t} \hat{a}_i^t \delta_{x_i^t} \tag{4}$$

where $\hat{a}_i^s$ and $\hat{a}_i^t$ are the probability masses that belong to the probability simplex, i.e., $\sum_{i=1}^{n_s} \hat{a}_i^s = 1$ and $\sum_{i=1}^{n_t} \hat{a}_i^t = 1$. Here, Kantorovich formulation [42] is adopted to compute the optimal coupling $\gamma^\star$ between $\widehat{P}_s$ and $\widehat{P}_t$ as follows:

$$\gamma^\star = \arg\min_{\gamma \in \mathcal{B}} \ \langle \gamma, C \rangle_F \tag{5}$$

where $\langle \cdot, \cdot \rangle_F$ is the Frobenius dot product, C is the cost matrix, whose term $C(i, j) = c(x_i^s, x_j^t)$ denotes the cost to move a probability mass from x_i^s to x_j^t, and $\mathcal{B}$ is the set of probabilistic couplings between $\widehat{P}_s$ and $\widehat{P}_t$

$$\mathcal{B} = \{\gamma \in (\mathbb{R}^+)^{n_s \times n_t} | \gamma \mathbf{1}_{n_t} = \widehat{P}_s, \gamma^{\mathbf{T}} \mathbf{1}_{n_s} = \widehat{P}_t\} \tag{6}$$

where $\mathbf{1}_n$ is a n-dimensional vector of ones.

The probability mass of each location in the target distribution should be set according to geographic phenomena, but it is difficult to obtain such information during an event. Therefore, in [31], it is assumed that the probability mass of locations in $\widehat{P}_s$ and $\widehat{P}_t$ is both subject to a uniform distribution, i.e., the probability mass of x_i^s and x_j^t is, respectively, $(1/n_s)$ and $(1/n_t)$. Then, the OT function T_{OT} can be expressed as

$$T_{\text{OT}}(x_i^s) = \sum_{j=1}^{n_t} n_s \gamma^\star(i, j) x_j^t. \tag{7}$$

Fig. 2 shows a graphical illustration of OT from the viewpoint of representation alignment. There are four source elements (in red) and four target elements (in blue). As it can be observed, the realigned elements (in red dashed circles) are well adapted to the targets, which is consistent with (7), in the sense that a source element could be transported to the target domain (however, only from a representation viewpoint). From (7), we can conclude that an element is likely to be transported to a location weighted by some target elements, which may not be in the target domain. For further analysis, we demonstrate the same domain adaption results in Fig. 2 in the sense of elements' geolocation, as shown in Fig. 3. As it can be noticed (again) in this example, there are two "A" elements in the source domain denoting the same geographical phenomenon. In the target domain, there is a "D" element without a corresponding collection in the source domain. From Fig. 3, we can conclude that one element "A" is relocated to the target domain, which is correctly aligned from the geolocation viewpoint and the representation viewpoint. The other "A" and "B" elements are correctly realigned to targets from a representation viewpoint; however, these same elements are wrongly relocated from a geolocation viewpoint. Another observation is that element "C" in the source is relocated to a location weighted by the targets {"B," "C"}, which is outside the target domain. This happens due to the fact that under the assumption of a uniform distribution, it is supposed that the elements in the source domain would be transported to the target domain with equal probability, that is, following a balanced distribution in the target domain. The achievement of such a balanced distribution may lead to two issues. First of all, part of the densely distributed elements might need to be transported to very far locations, which is not reasonable in practice. Another issue is that the areas with few data producers would be relocated with more data. In other words, the source data might be transported to a location within an inappropriate distance. In summary, the main problems of using OT when aligning geolocations are: 1) the transport might be outside the target domain and 2) the source data might be inappropriately transported.

C. Geographic Optimal Transport

As discussed before, the assumption of probability masses used in OT may restrict its application in geolocation alignment. To address this limitation, we introduce a new method called GOT, which aims at simultaneously aligning representations and geolocations in the context of heterogeneous geographic data fusion. Recall that $c(x_i^s, x_j^t)$ denotes the cost to move a probability mass from x_i^s to x_j^t. The GOT function is given as follows:

$$T_{\text{GOT}}\left(x_i^s\right) = \arg\min_{x_j^t \in \widehat{P}_t} \ c\left(x_i^s, x_j^t\right). \tag{8}$$

As shown in (8), GOT directly transports a source element x_i^s to the location of a target element x_j^t with minimum cost, and all the data in the source elements are eventually transported to the locations of the target elements. Note that

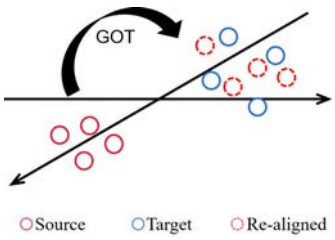

Fig. 4. Graphic illustration of GOT from the viewpoint of representation alignment, considering the same problem shown in Fig. 2.

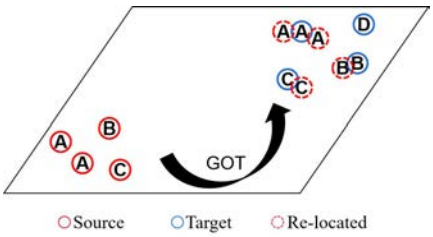

Fig. 5. Graphic illustration of GOT from the viewpoint of geolocation alignment, considering the same problem shown in Fig. 3.

this is the main difference between GOT and OT, as in OT elements may be transported to locations outside the target domain when aligning geolocations.

Furthermore, GOT has no assumption regarding the probability masses of domains. The transport is uniquely controlled by the cost $c(x_i^s, x_j^t)$. Therefore, there is a possibility that many elements may be transported to the same location and that no elements are transported to some locations. This is reasonable, as discussed before, since a location with more producers is likely to have more data, while a location with fewer ones probably has less data. For illustrative purposes, Figs. 4 and 5 show the graphical illustrations of the performance of GOT for the same problem previously described in Figs. 2 and 3, respectively. On the one hand, from the aspect of representation alignment (see Fig. 4), it can be observed that GOT can properly align elements from the source domain to the target domain. This behavior is very similar to that of OT. On the other hand, from the aspect of geolocation alignment, the performance of GOT is remarkable since all the source elements are correctly relocated to their corresponding targets (as shown in Fig. 5). Note that another important characteristic of GOT is that the two "A" elements from the source are transported to the same "A" location in the target. This property is essential as, in reality, it is possible that one single phenomenon is associated with many social media producers, that is, it is possible that many elements in the source correspond to the same target phenomenon. Again, this stands out as the main difference between GOT and OT: that GOT considers geolocations and representations simultaneously, where OT only considers the representations.

As mentioned before, GOT is fully controlled by the cost $c(x_i^s, x_j^t)$, leading to the possibility that many elements are transported to the same location. Although this may possibly happen, this may lead to the issue that producers from similar locations, indicating that different targets may be transported to the same location, resulting in an underestimation of the geographic extent in the target domain. In order to avoid this problem, let $O(x_j^t)$ be an overflow effect function denoting the total number of biased geographic data sources aligned to the same location in the target distribution. Let β be the overflow threshold. We define that if $O(x_j^t) \leq \beta$, x_i^s is transported to x_j^t. Otherwise, if $O(x_j^t) > \beta$, the overflowing data will be transported to the next minimum cost location. In practice, β can be determined by the quantity and aggregation degree of biased geographic data. In our experiments, we set β empirically to $n_s/1000$.

Note that, in this work, both OT and GOT are used for unsupervised domain adaptation purposes. Similar to OT, GOT also transports the source to the target. In summary, the main difference between them is that GOT can perform alignments of representation and geo-location simultaneously, whereas OT only aligns the domain representations, often resulting in wrong geolocation alignments.

D. Remote Sensing Features

In the fusion process, in addition to considering the distance factor, remote sensing features (capable of characterizing an event) are also added. For instance, in a flood event, it makes sense to use the well-known NDVI [31] that is based on the characteristics of water bodies, with low reflectance in the near-infrared bands and high reflectance in the red bands, and intended to enhance the contrast between land and water

$$\text{NDVI} = \frac{\rho(\text{NIR}) - \rho(\text{Red})}{\rho(\text{NIR}) + \rho(\text{Red})} \tag{9}$$

where $\rho(\text{NIR})$ and $\rho(\text{Red})$ are the surface reflectance of a near-infrared band (such as band 5 of Landsat 8 OLI imagery) and a red band (such as band 4 of Landsat 8 OLI imagery), respectively.

In order to characterize the flood more accurately, the difference between NDVI (before and after the flood event) is calculated, namely

$$\text{DIFF-NDVI} = \text{NDVI}_{t2} - \text{NDVI}_{t1} \tag{10}$$

where $t1$ and $t2$ are the times before and after the flood event, respectively. Such DIFF-NDVI exploits an important characteristic; the NDVI values of water bodies are smaller than those of other land types (generally, NDVI values of water bodies, cloud, and snow are negative), resulting in a decrease of NDVI in flooded areas.

Besides, the NDWI during or after the flood event can also be used to monitor a flood event [30], [43]

$$\text{NDWI} = \frac{\rho(\text{Green}) - \rho(\text{MIR})}{\rho(\text{Green}) + \rho(\text{MIR})} \tag{11}$$

where $\rho(\text{Green})$ and $\rho(\text{MIR})$ are the surface reflectance of a green band (such as band 3 of Landsat 8 OLI imagery) and a midinfrared band (such as band 6 of Landsat 8 OLI imagery), respectively.

Compared with the NDVI, NDWI can also reduce background noise [44] and better distinguish between water bodies and buildings. This is because both water bodies and floods have great NDWI values during (or after) the flood event.

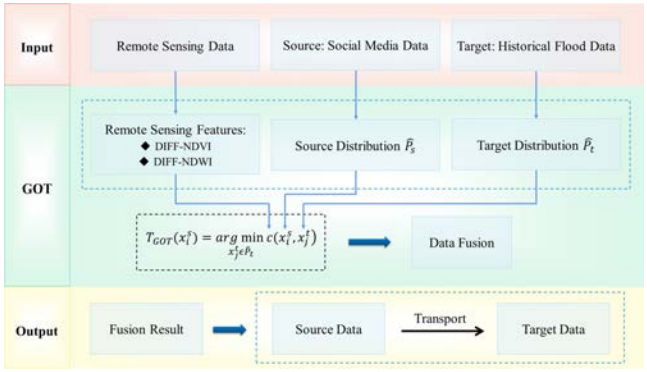

Fig. 6. Schematic overview of GOT for the fusion of heterogeneous remote sensing and social media data.

However, in this case, water bodies might be identified as floods when using NDWI. Therefore, we introduce a new form of NDWI to characterize the floods. Let

$$\text{DIFF-NDWI} = \text{NDWI}_{t2} - \text{NDWI}_{t1} \tag{12}$$

be the NDWI difference between the two times of $t1$ and $t2$, with the time stamp $t_2 > t_1$. Such DIFF-NDWI exploits an important characteristic; the NDWI values of water bodies are greater than those of other land types, resulting in an increase of NDWI in flooded areas.

Finally, it should be pointed out that the value ranges of both DIFF-NDVI and DIFF-NDWI are $[-2, 2]$. With this in mind, we can infer the following.

1) When DIFF-NDVI is close to -2, the area is more likely to be inundated.
2) When DIFF-NDWI is close to 2, the same observations as those for DIFF-NDVI $\rightarrow -2$ can be made.

E. Data Fusion

In this work, we propose a new data fusion model based on GOT by using the aforementioned remote sensing features as follows:

$$\begin{aligned} c(x_i^s, x_j^t) = &\left\|x_i^s - x_j^t\right\|_2^2 \\ &+ \alpha\left\|2 - \text{DIFF-NDWI}\left(x_j^t\right)\right\|_2^2 \\ &+ \alpha\left\|(-2) - \text{DIFF-NDVI}\left(x_j^t\right)\right\|_2^2 \end{aligned} \tag{13}$$

where α is a parameter that can be tuned by observing the distance transport cost in D, which is set to $1/5000$ in our experiments. As shown in (13), for the transport cost, the proposed function considers the squared Euclidean distance between x_i^s and x_j^t and two kinds of remote sensing features, i.e., DIFF-NDWI and DIFF-NDVI, bounded by extreme inundated scenarios, with the ultimate goal of transporting sources from dry to flooded areas within a relatively small distance.

For illustrative purposes, Fig. 6 shows a schematic flowchart of GOT for the fusion of heterogeneous remote sensing and social media data. As it can be observed, GOT is used to fuse remote sensing data, social media data, and historical flood data, resulting in the fact that the social media data are transported to the target data.

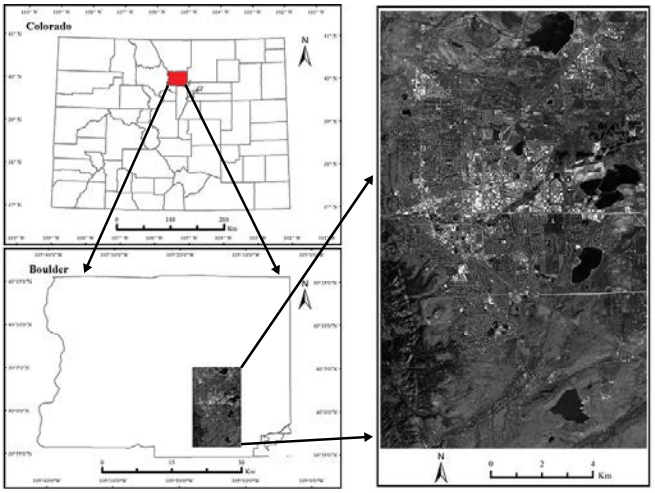

Fig. 7. Study area and its location in Boulder and Colorado.

IV. Data Sets

During September 9–16, 2013, a large-scale rainstorm occurred in a broad region of the Colorado Front Range foothills (and adjacent plains). The average annual precipitation was reached in just eight days, with local precipitation exceeding 17.7 in (450 mm). The flood (caused by extreme rainstorms) is still the most serious hydrological disaster in Colorado history. It stretched nearly 200 mi from north to south along the Colorado Front Range mountains, affecting 18 counties. The disaster killed eight people, lead to the evacuation of more than 180 000 people, and caused more than $2 billion in property losses. Such unprecedented catastrophe was caused by a combination of factors, including long duration of rainstorms, widespread spatial flood extent, and prolonged duration of flooding from days to weeks, before the finalization of rainstorms.

Located near the foothills of the Rocky Mountains, Boulder was at the center of the flood event and was the worst hit among the 18 counties affected by the disaster [26]. Compared with the average annual precipitation (20.7 in, 525 mm) in Boulder County, the daily precipitation on September 12 and 15 reached 9.08 in (231 mm) and 17 in (430 mm), respectively. In this catastrophic flood event, Boulder County confirmed three deaths and evacuated more than 1600 people, with 262 homes destroyed and nearly 300 more damaged. The flood damaged nearly 900 mi^2, of which more than 150 mi of roads were totally destroyed. The satellite images, social media data, historical flood data, and ground-truth data involved in this catastrophic flood event are all publicly available, providing a unique opportunity for the evaluation of our methodology. For this reason, we use the 2013 flood event in Boulder County as our case study for subsequent analysis (see Fig. 7).

A. Remote Sensing Data

Remote sensing is a reliable and synchronous method to capture spatiotemporal characteristics of an event [45], [46]. Our study comprises two Landsat 8 OLI images (path/row: 33/32), which are publicly available from the United States

Geological Survey (USGS) website.[1] Landsat 8 OLI includes nine bands with an imaging width of 185 × 185 km, with spatial resolution of 30 m, including a 15-m panchromatic band.

In this study, we select the multispectral Landsat 8 OLI images obtained on May 12 and September 17, 2013, to provide reliable remote sensing data before and after the flood event, respectively. These images are publicly available with fine spatial resolution, which can be used to extract the remote sensing features required for our study. As mentioned before, the floods in this catastrophic event continued for a period of time after the cessation of rainstorms. Therefore, the image of September 17, 2013, can better represent the spatial characteristics of flood events. Boulder was completely cloud-free in these two images, so high-quality optical remote sensing data can be obtained. This research uses Landsat 8 Level-1TP data products, which have undergone systematic radiation correction and geometric correction incorporating ground control points while employing a digital elevation model (DEM) for topographic displacement. Due to the absorption and scattering of atmospheric molecules, water vapor, aerosol, and other atmospheric components, satellite sensors receive mixed information on the interaction between the land surface and the atmosphere. In order to obtain the real land surface reflectance, we use the Fast Line-of-sight Atmospheric Analysis of Spectral Hypercubes (FLAASH) algorithm for atmospheric correction [47]. Then, the NDVI and NDWI (used to characterize water bodies in this study) can be calculated.

B. Social Media Data

As one of the largest social media sites, Twitter is a microblogging service that enables its users to send and receive short messages through the web, instant messaging, or SMS interfaces. These messages are called tweets [48]. Due to the real-time nature of Twitter, it can improve situational awareness and emergency response capability through the tweets issued by official government agencies and the public, in order to make wise decisions (especially during disasters [49]). Twitter users can search and filter interesting topic messages through hashtags, prefixed with the sign #. For example, hashtags #boulderflood and #coflood are used to represent the shared information about the Boulder flood event and the Colorado flood event, respectively. Twitter is particularly prominent in emergency response because it is able to search and store tweets related to disasters by combining Web tools or application program interfaces (APIs) using hashtags, as well as text and spatiotemporal constraints [26], [50]. Following [26], a total of 2254 tweets, which were harvested using Twitter APIs, extending from $105°18'2''$ to $105°10'40''W$ and $39°55'54''$ to $40°5'8''N$ during the flood event, are used in this study. Experiments were performed using these Boulder's flood-related geotagged tweets during the flood event only. As mentioned earlier, geotagged tweets that indicate flood events tend to suffer from geolocation problems since users usually tweet from relatively safe places rather than directly on the flood sites. In our context, such biased geotagged tweets represent the source distribution for transport methods.

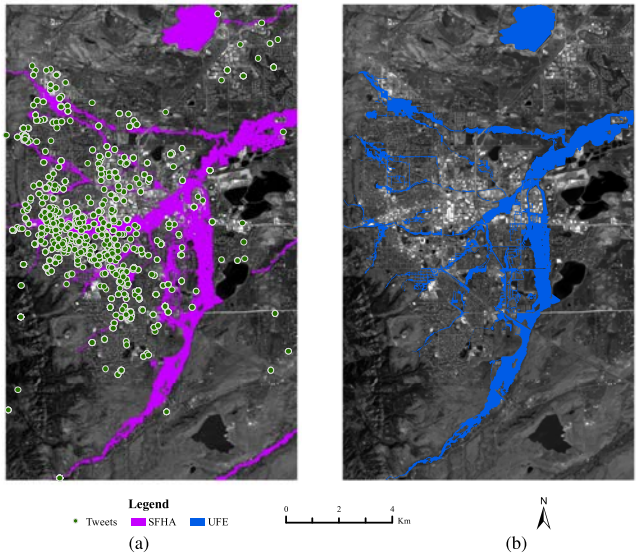

Fig. 8. Spatial distribution of the original tweets, history flood extent as prior information, and UFE as ground truth for the 2013 Boulder flood event. (a) Tweets and special flood hazard area. (b) Urban flood extent.

C. Historical Flood Data and Ground Truth

The Flood Insurance Rate Maps (FIRM) identifies areas in a community that is subject to flooding and shows the risks associated with these flood hazards. One of the areas shown on the FIRM is the Special Flood Hazard Area (SFHA), which is defined as the area that will be inundated by the flood event (having a 1% chance of being equaled or exceeded in any given year). The SFHA for Boulder Colorado is publicly available on the website of the Federal Emergency Management Agency,[2] which is referred to as the base flood or 100-year flood. Since the SFHA can be used as an effective means to collect historical flood data, this study sets it as the target distribution for the transport of biased geotagged tweets. The open data of urban flood extent (UFE) during the 2013 flood event can be downloaded from the website of Boulder city[3] and used as our ground truth to evaluate different methods for alignment. The UFE was collected by Boulder citizens, using handheld GPS devices and photographs from communities.

Fig. 8 shows the aforementioned Landsat 8 OLI data as the background image. The biased geotagged tweets along with the SFHA is shown in Fig. 8(a), while Fig. 8(b) shows the UFE. At this point, we emphasize that, on the one hand, the UFE is smaller than (or part of) the SFHA. This is expected, as the SFHA considered here is a 100-year floodplain, which is supposed to cover all flood possibilities that could happen in 100 years. On the other hand, UFE is very similar to SFHA. This means that the flood scale is very severe in the considered case. Finally, it should also be pointed

[1] http://www.earthexplorer.usgs.gov

[2] http://www.fema.gov

[3] http://www.bouldercolorado.gov

TABLE I
ACCURACY EVALUATION OF RELOCATED TWEETS USING DIFFERENT METHODS

Method	TP	FP	P	Time(s)
None	269	1985	11.93%	-
OT	1341	913	59.49%	208
GOT	1518	736	**67.35%**	16

out that the data fusion aims at relocating the biased geotagged tweets to the UFE, with the SFHA being the prior source of flood information.

V. RESULTS

In this section, we first perform a quantitative evaluation of the precision results of relocated tweets using different methods for the 2013 Boulder flood event. Then, the spatial distributions and transport paths of relocated tweets are discussed. In addition, we further explore the practical performance of the proposed GOT and OT using a new metric, named corrected precision (P_c).

A. Quantitative Evaluation

Before presenting our quantitative results, we introduce the metrics considered for evaluation.

1) "TP" denotes the number of relocated tweets that fall within the UFE, i.e., the ground truth (true positives).
2) "FP" denotes the number of relocated tweets that fall outside the UFE, i.e., the ground truth (false positives).
3) "P" denotes the proportion of TPs, which is given by: $P = \mathrm{TP}/(\mathrm{TP} + \mathrm{FP})$.

In this section, we first present a quantitative evaluation of the results obtained by the proposed GOT. For comparative purposes, the results obtained by the method in [31] (using OT) are also reported. For simplicity, hereinafter, we use GOT and OT to denote the proposed method and the method in [31], respectively. Table I shows the obtained results in terms of accuracy. Concerning P, several conclusions can be obtained from Table I. First of all, it is remarkable that the proposed GOT obtained much better results than those obtained by OT. Furthermore, regarding the running time (in seconds), GOT only spent 16 s, which is much faster that OT (208 s). This is because GOT avoids learning the overall coupling for all elements, therefore behaving more efficiently.

B. Qualitative Illustration

Here, we present a graphical comparison of the maps obtained by the proposed GOT and OT. Fig. 9 shows the two maps. It can be observed that the relocated tweets in the GOT map are more concentrated in the UFE, whereas in the OT map, they are more uniformly distributed throughout the UFE. This means that there are many tweets transported to the same location in the GOT map, whereas in the OT map, tweets are transported to different locations. This is consistent with the mechanism that GOT and OT hold. Specifically, GOT allows multiple tweets to be transported to the same location. However, OT assumes that the probability masses of locations

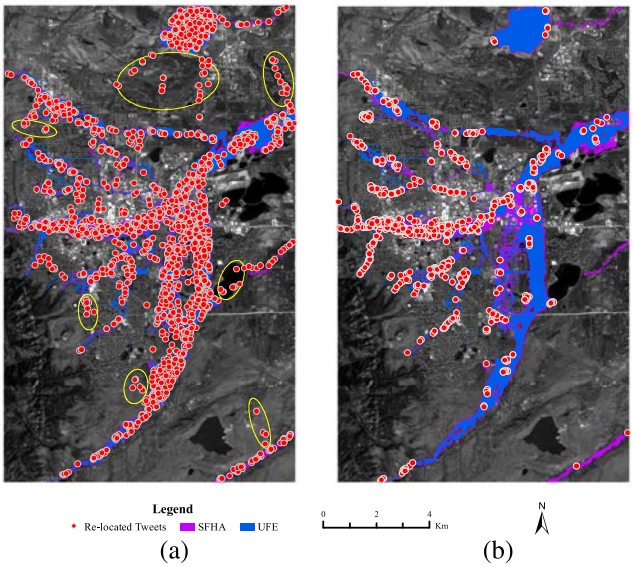

Fig. 9. Results obtained by (a) OT and (b) GOT.

in SFHA are subjected to a uniform distribution. The relocated tweets are consequentially uniformly distributed. It should be noted, again, that (in reality) the GOT mechanism is more reasonable since it is possible that many people tweet from the same flooded area. Furthermore, it is also important to point out that GOT aligned all the tweets into the target domain, i.e., SFHA; however, OT transported some of the tweets to locations outside of the SFHA, as marked by the yellow ellipses. It is critical from a theoretical viewpoint that all the sources should be aligned to the target domain. From a practical viewpoint, the SFHA (as a 100-year base) is supposed to cover the full UFE, which is true in our case (all alignments should also be inside the SFHA).

In order to further illustrate the performance of GOT and OT in more detail, we select two groups of tweets, with 252 and 226 tweets, respectively. Both groups are located near the UFE through their transport paths. The idea is to analyze the behavior of the two methods, as shown in Fig. 10. First of all, it can be observed that [as that shown in Fig. 9(a)] in OT, tweets are likely to be transported to different locations, whereas in GOT, there are different tweets being transported to the same (or a similar) location [see Fig. 9(b)]. Again, this is consistent with the mechanisms that the two methods hold. A most important aspect is that, in GOT, tweets are transported to the UFE at a close distance, which is entirely reasonable. However, in OT, these tweets are mostly transported to very far locations. This is a very interesting point. From a global viewpoint, for both GOT and OT, the tweets are mostly correctly relocated to flooded areas. However, it is easy to tell that the relocations of OT are mostly wrong, due to the fact that it is unlikely for tweeters to tweet from a very far distance.

C. Further Analysis

In order to further analyze this behavior, we introduce a new metric, namely "P_c" (corrected precision), to denote the

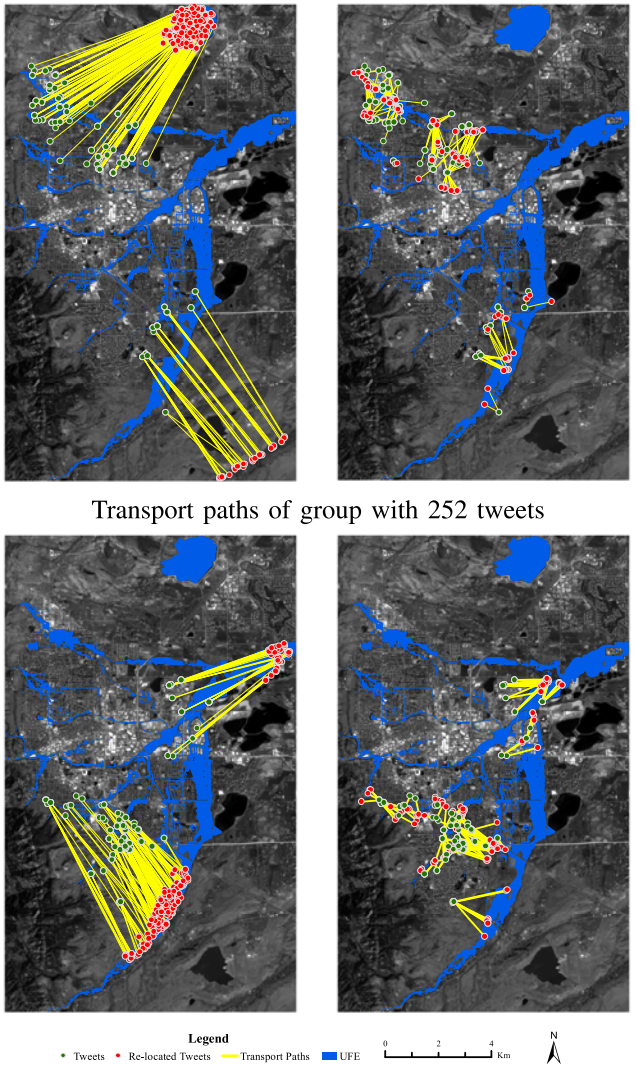

Fig. 10. Graphical illustration of the transport paths of two groups of tweets: OT (left) and GOT (right).

TABLE II

CORRECTED PRECISION OF RELOCATED TWEETS BY OT AND GOT FOR THE TWO GROUPS OF TWEETS IN FIG. 10

Group	Method	P	P_c
Group1	OT	82.54%	0%
	GOT	83.63%	56.11%
Group2	OT	77.43%	0%
	GOT	82.74%	44.69%

proportion of relocated tweets being transported to the UFE with a transport distance less than a given distance, i.e., 1 km, in our study. Due to the fact that it is very difficult (and of less interest) for tweeters to tweet from a location that is quite far, we are aware that a closer distance, for instance, 100 m, would be more reasonable. However, after considering the spatial resolution of the Landsat 8 OLI image, in this flood event, we empirically set 1 km for our study.

Table II shows the obtained results for the two groups of tweets in Fig. 10. It can be observed that both GOT and OT obtained very good performance with respect to P. This is expected, according to the analysis on Fig. 10 in Section V-B, as in Fig. 10, most of the tweets are relocated to the UFE. However, if we look into the corrected precision values, P_c, it is completely the other way around. P_c of OT is 0% in both groups. This means that all tweets are transported to locations with distances far from 1 km or outside the UFE. This, in practice, can be considered as a wrong relocation. It should be pointed out that the performance of GOT is still remarkable under this condition. However, the obtained values of P_c are much worse than P, also for GOT.

TABLE III

CORRECTED PRECISION OF RELOCATED TWEETS FROM OT AND GOT FOR THE WHOLE DATA SET

Method	P	P_c
OT	59.49%	1.20%
GOT	67.35%	45.61%

In order to have a better evaluation of the corrected precision, Table III shows the obtained P_c values for the whole data set. If we compare Tables II and III, the difference is that, in the latter, P is worse than in the former. This is reasonable, as the groups in Fig. 10 are selected with tweets that are well relocated to the UFE. An interesting aspect is the similar observations that can be made from these two tables. First of all, as expected, P_c is worse than P for both OT and GOT. Furthermore, for OT, in both tables, P_c is quite bad. This means that almost no tweets are correctly relocated. Finally, for the proposed GOT, the performance of P_c is remarkable. A very important point is that, for GOT, the corrected precision P_c is very similar for the whole data set and the individual groups. In the end, we can conclude that GOT is quite robust with respect to the corrected precisions.

VI. CONCLUSION AND FUTURE RESEARCH

In this article, we introduce a new fusion method for heterogeneous geographic data that are able to align representations and geolocations simultaneously. Taking a 2013 Boulder flood event as a case study, we apply our GOT method to solve problems involved in the fusion of remote sensing and social media data. Taking a flood event as an example, we introduced some remote sensing features derived from water indicators, i.e., the NDVI and NDWI, and further exploited them in the fusion task. According to our experiments, GOT can successfully align spatially biased geotagged social media data to the areas of the event, with high precision and stable performance. In future research, our fusion of heterogeneous geographic data will consider additional data sources, including content and pictures coming from social media, and synthetic aperture radar data.

ACKNOWLEDGMENT

The authors gratefully thank Dr. Guido Cervone for his generosity in providing Twitter data related to the considered case study.

REFERENCES

[1] C. He, B. Gao, Q. Huang, Q. Ma, and Y. Dou, "Environmental degradation in the urban areas of China: Evidence from multi-source remote sensing data," *Remote Sens. Environ.*, vol. 193, pp. 65–75, May 2017.

[2] J. Li *et al.*, "Social media: New perspectives to improve remote sensing for emergency response," *Proc. IEEE*, vol. 105, no. 10, pp. 1900–1912, Oct. 2017.

[3] Q. Huang, G. Cervone, and G. Zhang, "A cloud-enabled automatic disaster analysis system of multi-sourced data streams: An example synthesizing social media, remote sensing and wikipedia data," *Comput., Environ. Urban Syst.*, vol. 66, pp. 23–37, Nov. 2017.

[4] G. Boni *et al.*, "A prototype system for flood monitoring based on flood forecast combined with COSMO-SkyMed and Sentinel-1 data," *IEEE J. Sel. Topics Appl. Earth Observ. Remote Sens.*, vol. 9, no. 6, pp. 2794–2805, Jun. 2016.

[5] N. Courty, R. Flamary, D. Tuia, and A. Rakotomamonjy, "Optimal transport for domain adaptation," *IEEE Trans. Pattern Anal. Mach. Intell.*, vol. 39, no. 9, pp. 1853–1865, Sep. 2017.

[6] S. J. Pan and Q. Yang, "A survey on transfer learning," *IEEE Trans. Knowl. Data Eng.*, vol. 22, no. 10, pp. 1345–1359, Oct. 2010.

[7] R. I. Ogie and H. Forehead, "Investigating the accuracy of georeferenced social media data for flood mapping: The PetaJakarta. org case study," in *Proc. 4th Int. Conf. Inf. Commun. Technol. Disaster Manage. (ICT-DM)*, Dec. 2017, pp. 1–6.

[8] A. Acar and Y. Muraki, "Twitter for crisis communication: Lessons learned from Japan's tsunami disaster," *Int. J. Web Based Commun.*, vol. 7, no. 3, pp. 392–402, Jul. 2011.

[9] J. Hoffman, E. Rodner, J. Donahue, T. Darrell, and K. Saenko, "Efficient learning of domain-invariant image representations," in *Proc. Int. Conf. Learn. Represent.*, 2013, pp. 1–9.

[10] K. Saenko, B. Kulis, M. Fritz, and T. Darrell, "Adapting visual category models to new domains," in *Proc. Eur. Conf. Comput. Vis.*, 2010, pp. 213–226.

[11] B. Kulis, K. Saenko, and T. Darrell, "What you saw is not what you get: Domain adaptation using asymmetric kernel transforms," in *Proc. IEEE Conf. Comput. Vis. Pattern Recognit.*, Jun. 2011, pp. 1785–1792.

[12] S. J. Pan, I. W. Tsang, J. T. Kwok, and Q. Yang, "Domain adaptation via transfer component analysis," *IEEE Trans. Neural Netw.*, vol. 22, no. 2, pp. 199–210, Feb. 2011.

[13] J. Zheng, M. Liu, R. Chellappa, and P. J. Phillips, "A Grassmann manifold-based domain adaptation approach," in *Proc. 21st Int. Conf. Pattern Recognit.*, 2012, pp. 2095–2099.

[14] B. Gong, Y. Shi, F. Sha, and K. Grauman, "Geodesic flow kernel for unsupervised domain adaptation," in *Proc. IEEE Conf. Comput. Vis. Pattern Recognit.*, Jun. 2012, pp. 2066–2073.

[15] N. Courty, R. Flamary, and D. Tuia, "Domain adaptation with regularized optimal transport," in *Proc. Joint Eur. Conf. Mach. Learn. Knowl. Discovery Databases*, 2014, pp. 274–289.

[16] I. Redko, A. Habrard, and M. Sebban, "Theoretical analysis of domain adaptation with optimal transport," in *Proc. Joint Eur. Conf. Mach. Learn. Knowl. Discovery Databases*, 2017, pp. 737–753.

[17] L. M. Fonseca and B. S. Manjunath, "Registration techniques for multisensor remotely sensed imagery," *Photogramm. Eng. Remote Sens.*, vol. 62, no. 9, pp. 1049–1056, Sep. 1996.

[18] Y. Li, J. Li, L. He, J. Chen, and A. Plaza, "A new sensor bias-driven spatio-temporal fusion model based on convolutional neural networks," *Sci. China Inf. Sci.*, vol. 63, no. 4, Apr. 2020, Art. no. 140302.

[19] J. Li, Y. Li, L. He, J. Chen, and A. Plaza, "Spatio-temporal fusion for remote sensing data: An overview and new benchmark," *Sci. China Inf. Sci.*, vol. 63, no. 4, Apr. 2020, Art. no. 140301.

[20] M. Claverie *et al.*, "The harmonized Landsat and Sentinel-2 surface reflectance data set," *Remote Sens. Environ.*, vol. 219, pp. 145–161, Dec. 2018.

[21] D. Dimov, J. Kuhn, and C. Conrad, "Assessment of cropping system diversity in the Fergana Valley through image fusion of Landsat 8 and Sentinel-1," *ISPRS Ann. Photogramm., Remote Sens. Spatial Inf. Sci.*, vol. 3, p. 173, 2016.

[22] M. F. Goodchild, "Citizens as sensors: The world of volunteered geography," *GeoJournal*, vol. 69, no. 4, pp. 211–221, Nov. 2007.

[23] Z. Ashktorab, C. Brown, M. Nandi, and A. Culotta, "Tweedr: Mining Twitter to inform disaster response," in *Proc. Int. Conf. Inf. Syst. Crisis Response Manage.*, 2014, pp. 269–272.

[24] J. B. Houston *et al.*, "Social media and disasters: A functional framework for social media use in disaster planning, response, and research," *Disasters*, vol. 39, no. 1, pp. 1–22, Jan. 2015.

[25] E. Schnebele, C. Oxendine, G. Cervone, C. M. Ferreira, and N. Waters, "Using non-authoritative sources during emergencies in urban areas," in *Computational Approaches for Urban Environments*. Cham, Switzerland: Springer, 2015, pp. 337–361.

[26] G. Cervone, E. Sava, Q. Huang, E. Schnebele, J. Harrison, and N. Waters, "Using Twitter for tasking remote-sensing data collection and damage assessment: 2013 boulder flood case study," *Int. J. Remote Sens.*, vol. 37, no. 1, pp. 100–124, Jan. 2016.

[27] E. Schnebele, G. Cervone, S. Kumar, and N. Waters, "Real time estimation of the calgary floods using limited remote sensing data," *Water*, vol. 6, no. 2, pp. 381–398, Feb. 2014.

[28] X. Huang, C. Wang, and Z. Li, "A near real-time flood-mapping approach by integrating social media and post-event satellite imagery," *Ann. GIS*, vol. 24, no. 2, pp. 113–123, Apr. 2018.

[29] B. Jongman, J. Wagemaker, B. Romero, and E. de Perez, "Early flood detection for rapid humanitarian response: Harnessing near real-time satellite and Twitter signals," *ISPRS Int. J. Geo-Inf.*, vol. 4, no. 4, pp. 2246–2266, 2015.

[30] G. Panteras and G. Cervone, "Enhancing the temporal resolution of satellite-based flood extent generation using crowdsourced data for disaster monitoring," *Int. J. Remote Sens.*, vol. 39, no. 5, pp. 1459–1474, 2018.

[31] H. Wang, E. Skau, H. Krim, and G. Cervone, "Fusing heterogeneous data: A case for remote sensing and social media," *IEEE Trans. Geosci. Remote Sens.*, vol. 56, no. 12, pp. 6956–6968, Dec. 2018.

[32] D. Tuia and G. Camps-Valls, "Kernel manifold alignment for domain adaptation," *PLoS ONE*, vol. 11, no. 2, Feb. 2016, Art. no. e0148655.

[33] C. Wang and S. Mahadevan, "Heterogeneous domain adaptation using manifold alignment," in *Proc. Int. Joint Conf. Artif. Intell. (IJCAI)*, 2011, vol. 22, no. 1, p. 1541.

[34] I.-H. Jhuo, D. Liu, D. T. Lee, and S.-F. Chang, "Robust visual domain adaptation with low-rank reconstruction," in *Proc. IEEE Conf. Comput. Vis. Pattern Recognit.*, Jun. 2012, pp. 2168–2175.

[35] C. Wang and S. Mahadevan, "Manifold alignment without correspondence," in *Proc. Int. Joint Conf. Artif. Intell. (IJCAI)*, 2009, p. 3.

[36] M. Long, H. Zhu, J. Wang, and M. I. Jordan, "Unsupervised domain adaptation with residual transfer networks," in *Proc. Adv. Neural Inf. Process. Syst.*, 2016, pp. 136–144.

[37] M. Baktashmotlagh, M. T. Harandi, B. C. Lovell, and M. Salzmann, "Unsupervised domain adaptation by domain invariant projection," in *Proc. IEEE Int. Conf. Comput. Vis.*, Dec. 2013, pp. 769–776.

[38] R. Gopalan, R. Li, and R. Chellappa, "Domain adaptation for object recognition: An unsupervised approach," in *Proc. Int. Conf. Comput. Vis.*, Nov. 2011, pp. 999–1006.

[39] K. Saito, K. Watanabe, Y. Ushiku, and T. Harada, "Maximum classifier discrepancy for unsupervised domain adaptation," in *Proc. IEEE/CVF Conf. Comput. Vis. Pattern Recognit.*, Jun. 2018, pp. 3723–3732.

[40] X. Wei, H. Li, J. Sun, and L. Chen, "Unsupervised domain adaptation with regularized optimal transport for multimodal 2D+3D facial expression recognition," in *Proc. 13th IEEE Int. Conf. Automat. Face Gesture Recognit. (FG)*, May 2018, pp. 31–37.

[41] Y. Yan, W. Li, H. Wu, H. Min, M. Tan, and Q. Wu, "Semi-supervised optimal transport for heterogeneous domain adaptation," in *Proc. 27th Int. Joint Conf. Artif. Intell.*, Jul. 2018, pp. 2969–2975.

[42] L. V. Kantorovich, "On the translocation of masses," *J. Math. Sci.*, vol. 133, no. 4, pp. 1381–1382, Mar. 2006.

[43] J. F. Rosser, D. G. Leibovici, and M. J. Jackson, "Rapid flood inundation mapping using social media, remote sensing and topographic data," *Natural Hazards*, vol. 87, no. 1, pp. 103–120, May 2017.

[44] H.-Q. Xu, "A study on information extraction of water body with the modified normalized difference water index (MNDWI)," *J. Remote Sens.*, vol. 9, pp. 589–595, Sep. 2005.

[45] K. E. Joyce, S. E. Belliss, S. V. Samsonov, S. J. McNeill, and P. J. Glassey, "A review of the status of satellite remote sensing and image processing techniques for mapping natural hazards and disasters," *Prog. Phys. Geogr., Earth Environ.*, vol. 33, no. 2, pp. 183–207, Apr. 2009.

[46] N. Kussul, S. Skakun, A. Y. Shelestov, O. Kussul, and B. Yailymov, "Resilience aspects in the sensor Web infrastructure for natural disaster monitoring and risk assessment based on Earth observation data," *IEEE J. Sel. Topics Appl. Earth Observ. Remote Sens.*, vol. 7, no. 9, pp. 3826–3832, Sep. 2014.

[47] T. Cooley *et al.*, "FLAASH, a MODTRAN4-based atmospheric correction algorithm, its application and validation," in *Proc. IEEE Int. Geosci. Remote Sens. Symp. (IGARSS)*, vol. 3, Jun. 2002, pp. 1414–1418.

[48] N. Waters, "Social network analysis," in *Handbook of Regional Science*. Berlin, Germany: Springer, 2014, pp. 725–740.

[49] E. Tobias, "Using Twitter and other social media platforms to provide situational awareness during an incident," *J. Bus. Continuity Emergency Planning*, vol. 5, no. 3, pp. 208–223, 2011.

[50] S. Vieweg, A. L. Hughes, K. Starbird, and L. Palen, "Microblogging during two natural hazards events: What Twitter may contribute to situational awareness," in *Proc. SIGCHI Conf. Hum. Factors Comput. Syst.*, 2010, pp. 1079–1088.

Zhenjie Liu (Member, IEEE) received the B.S. and M.E. degrees from South China Agricultural University, Guangzhou, China, in 2016 and 2019, respectively. He is pursuing the Ph.D. degree with Sun Yat-sen University, Guangzhou.

His research interests include the fusion of remote sensing and social media, and urban flood mapping.

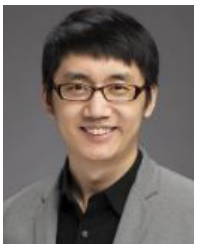

Qiang Qiu received the B.S. degree in software engineering from Shandong University, Jinan, China, in 2010, and the Ph.D. degree in computer application technology from the University of Chinese Academy of Sciences, Beijing, China, in 2015.

He is an Engineer with the CAS Key Laboratory on Network Data Science and Technology, Institute of Computing Technology, Chinese Academy of Sciences (CAS), Beijing. He has published over 20 articles in his major and has rich project experiments, including the National Science Foundation for Young Scientists of China, the National High-tech RESEARCH AND DEVELOPMENT Program (863 Program) of China, and the National Major Projects of China. His research interests include big data mining, spatial data analysis, geographic information system, and parallel computing.

Jun Li (Senior Member, IEEE) received the B.S. degree in geographic information systems from Hunan Normal University, Changsha, China, in 2004, the M.E. degree in remote sensing from Peking University, Beijing, China, in 2007, and the Ph.D. degree in electrical engineering from the Instituto de Telecomunicações, Instituto Superior Técnico (IST), Universidade Técnica de Lisbon, Lisbon, Portugal, in 2011.

She is a Full Professor with Sun Yat-sen University, Guangzhou, China. Her main research interests comprise remotely sensed hyperspectral image analysis, signal processing, supervised/semisupervised learning, and active learning.

Dr. Li is the Editor-in-Chief of the IEEE JOURNAL OF SELECTED TOPICS IN APPLIED EARTH OBSERVATIONS AND REMOTE SENSING. She has been a Guest Editor for several journals, including the PROCEEDINGS OF THE IEEE and the *ISPRS Journal of Photogrammetry and Remote Sensing*.

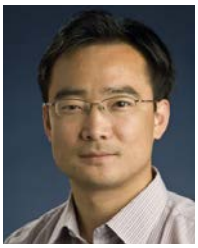

Lizhe Wang received the B.E. and M.E. degrees in electrical engineering and automation from Tsinghua University, Beijing, China, in 1998 and 2001, respectively, and the D.E. degree *(magna cum laude)* in applied computing science from the Karlsruhe Institute of Technology, Karlsruhe, Germany, in 2007.

He is the Dean and "ChuTian" Chair Professor with the School of Computer Science, China University of Geosciences, Wuhan, China. His research interests include remote sensing data processing, digital earth, and big data computing.

Dr. Wang is a Fellow of the Institution of Engineering and Technology and the British Computer Society. He was a recipient of the Distinguished Young Scholars of the National Natural Science Foundation of China, the National Leading Talents of Science and Technology Innovation, and the 100-Talents Program of the Chinese Academy of Sciences. He is also an Associate Editor of *Remote Sensing*, the *International Journal of Digital Earth*, *ACM Computing Surveys*, the IEEE TRANSACTIONS ON PARALLEL AND DISTRIBUTED SYSTEMS, and the IEEE TRANSACTIONS ON SUSTAINABLE COMPUTING.

Antonio Plaza (Fellow, IEEE) received the M.Sc. and Ph.D. degrees in computer engineering from the University of Extremadura, Cáceres, Spain, in 1999 and 2002, respectively.

He is the Head of the Hyperspectral Computing Laboratory, Department of Technology of Computers and Communications, University of Extremadura. He has authored more than 600 publications, including 200 JCR journal articles (145 in IEEE journals), 23 book chapters, and 285 peer-reviewed conference proceeding papers. He has guest edited ten special issues on hyperspectral remote sensing for different journals. His main research interests comprise hyperspectral data processing and parallel computing of remote sensing data.

Dr. Plaza was a member of the Editorial Board of the IEEE Geoscience and Remote Sensing Newsletter from 2011 to 2012 and the *IEEE Geoscience and Remote Sensing Magazine* in 2013 and the Steering Committee of the IEEE JOURNAL OF SELECTED TOPICS IN APPLIED EARTH OBSERVATIONS AND REMOTE SENSING (JSTARS). He is a fellow of IEEE for his contributions to hyperspectral data processing and parallel computing of Earth observation data. He was a recipient of the recognition of Best Reviewers of the IEEE Geoscience and Remote Sensing Letters in 2009 and the recognition of Best Reviewers of the IEEE TRANSACTIONS ON GEOSCIENCE AND REMOTE SENSING in 2010, for which he served as Associate Editor from 2007 to 2012. He was a recipient of the Best Column Award of the *IEEE Signal Processing Magazine* in 2015, the 2013 Best Paper Award of the JSTARS journal, and the most highly cited paper (2005–2010) in the *Journal of Parallel and Distributed Computing*. He received best paper awards at the IEEE International Conference on Space Technology and the IEEE Symposium on Signal Processing and Information Technology. He served as the Director of Education Activities for the IEEE Geoscience and Remote Sensing Society (GRSS) from 2011 to 2012 and the President of the Spanish Chapter, IEEE GRSS, from 2012 to 2016. He has reviewed more than 500 manuscripts for over 50 different journals. He is also an Associate Editor for IEEE ACCESS. He is also serving as the Editor-in-Chief for the IEEE TRANSACTIONS ON GEOSCIENCE AND REMOTE SENSING. Additional information: http://www.umbc.edu/rssipl/people/aplaza.